Geophysical Prospecting EAGE EUROPEAN ASSOCIATION OF GEOSCIENTISTS & ENGINEERS

Geophysical Prospecting, 2016 doi: 10.1111/1365-2478.12480

Perturbation-based moveout approximations in anisotropic media

Shibo Xu*, Alexey Stovas and Qi Hao

Department of Petroleum Engineering and Applied Geophysics, Norwegian University of Science and Technology, S.P. Andersens veg 15a, NO-7491 Trondheim, Norway

Received April 2016, revision accepted October 2016

ABSTRACT

The moveout approximations play an important role in seismic data processing. The standard hyperbolic moveout approximation is based on an elliptical background model with two velocities: vertical and normal moveout. We propose a new set of moveout approximations based on a perturbation series in terms of anellipticity parameters using the alternative elliptical background model defined by vertical and horizontal velocities. We start with a transversely isotropic medium with a vertical symmetry axis. Then, we extend this approach to a homogeneous orthorhombic medium. To define the perturbation coefficients for a new background, we solve the eikonal equation with horizontal velocities in transversely isotropic medium with a vertical symmetry axis and orthorhombic media. To stabilise the perturbation series and improve the accuracy, the Shanks transform is applied for all the cases. We select different parameterisations for both velocities and anellipticity parameters for an orthorhombic model. From the comparison in traveltime error, the new moveout approximations result in better accuracy comparing with the standard perturbation-based methods and other approximations.

Key words: Moveout approximation, Anisotropy, Seismic modelling.

INTRODUCTION

The moveout approximations are commonly used in seismic data processing such as velocity analysis, modelling and time migration. In isotropic or elliptical isotropic media, the moveout function has a hyperbolic form. We need to take non-hyperbolicity (driven by anellipticity) into consideration, as it commonly exists and plays an important role in seismic data processing and interpretation, especially for large offsets. The moveout function has a non-hyperbolic form in anisotropic media. Different non-hyperbolic moveout approximations for a homogeneous transversely isotropic medium with a vertical symmetry axis VTI are listed and discussed in Fowler (2003), Fomel (2004) and Golikov and Stovas (2012). Fomel and Stovas (2010) proposed the generalised non-hyperbolic moveout approximation (GMA) based on parameters computed from the zero-offset ray and one additional nonzero-offset ray. This approximation is very accurate and can be converted into other well-known approximations by the appropriate choice of the parameters. Alkhalifah (2011) proposed the traveltime expression with a series in terms of anelliptic parameter η by solving the eikonal equation for an acoustic VTI medium and by applying the Shanks transform to obtain higher accuracy.

The orthorhombic (ORT) model is introduced by Schoenberg and Helbig (1997) to describe fractured reservoirs and explains well the azimuthal dependency in surface seismic data. Tsvankin (1997, 2012) defined nine elastic model parameters for the ORT model that can be reduced to six parameters in an acoustic approximation (Alkhalifah 2003). In the group domain, we call the first-order curvatures the normal moveout (NMO) velocity ellipses (Grechka and Tsvankin 1999a,b) and the second-order curvatures the anellipticities as they represent the anelliptic behaviour for slowness or traveltime surface. Stovas (2015) derived the azimuthally dependent kinematic properties of the ORT media and defined the

*E-mail: shibo.xu@ntnu.no

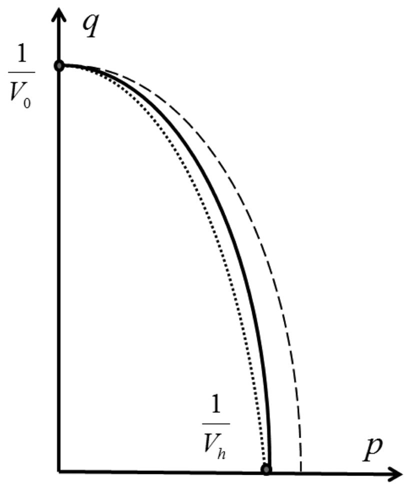

Figure 1 Slowness curve for the VTI model. p and q are the horizontal and vertical slowness, respectively. The exact approximation, the approximation by vertical velocity and NMO velocity and the approximation by vertical velocity and horizontal velocity are shown as solid, dashed and dotted lines, respectively.

effective ORT parameters in the Dix-type relation when there are azimuth variations between the multi-layers. Recently, Sripanich and Fomel (2015) proposed an anelliptic approximation for qP velocities in ORT media. A very accurate GMA approximation in ORT media for phase and group velocities is developed by Hao and Stovas (2016). The perturbation-based moveout approximation with a traditional elliptic background for ORT media is discussed by Stovas, Masmoudi and Alkhalifah (2016). The traveltime approximation for the ORT

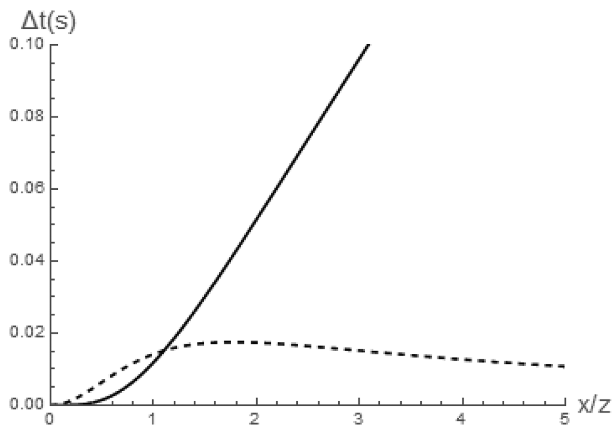

Figure 2 Traveltime error from hyperbolic moveout approximations using two background models in VTI media. The results using NMO and horizontal velocities are shown as solid and dashed lines, respectively.

model using perturbation theory by other anellipticity parameters in inhomogeneous background media is developed by Masmoudi and Alkhalifah (2016).

We develop a new perturbation-based moveout approximation based on an alternative background model in VTI and ORT models and apply the Shanks transform (Bender and Orszag 1978) to improve the accuracy. For a homogeneous ORT model, we select different parameterisations for both velocity background and anelliptic parameters.

New moveout approximation in a transversely isotropic medium with a vertical symmetry axis

To define the non-hyperbolic traveltime approximation for a VTI model, we select the hyperbolic traveltime background and anellipticity parameter η (Alkhalifah 1998), where $\eta = (\varepsilon - \delta)/(1 + 2\delta)$ with parameters δ and ε being the Thomsen anisotropy parameters (Thomsen 1986). In the standard case, one can use the Taylor series in offset for traveltime squared to obtain the moveout approximation. Alternatively, we can have more options to represent the traveltime function when using the perturbation series in terms of small model parameters. Alkhalifah (2011) proposed a moveout approximation based on the perturbation series in anellipticity parameter η, which is more accurate than the standard Taylor series in offset. In our approach, we follow the same idea. For a VTI model, compared with the ORT model, there is only one parameter that can be considered as the small one, namely, anellipticity parameter η.

To define the standard background model, we use two velocities: vertical velocity (or zero-offset traveltime) and NMO velocity. The classic moveout is given by the following hyperbolic equation:

$$t^2 \approx t_0^2 + \frac{x^2}{V_n^2}, \tag{1}$$

where t and t_0 are the traveltime and the vertical traveltime, respectively, x is the offset, and V_n is the NMO velocity. For a VTI model, $V_n = V_0\sqrt{1 + 2\delta}$, V_0 is the vertical velocity.

Alkhalifah (2011) proposed to expand the traveltime expression into a series in anelliptic parameter η by solving the eikonal equation (Alkhalifah 2000):

$$V_n^2 (1 + 2\eta) \left(\frac{\partial \tau}{\partial x}\right)^2 + V_0^2 \left(\frac{\partial \tau}{\partial z}\right)^2 - 2\eta V_n^2 V_0^2 \left(\frac{\partial \tau}{\partial x}\right)^2 \left(\frac{\partial \tau}{\partial z}\right)^2 = 1. \tag{2}$$

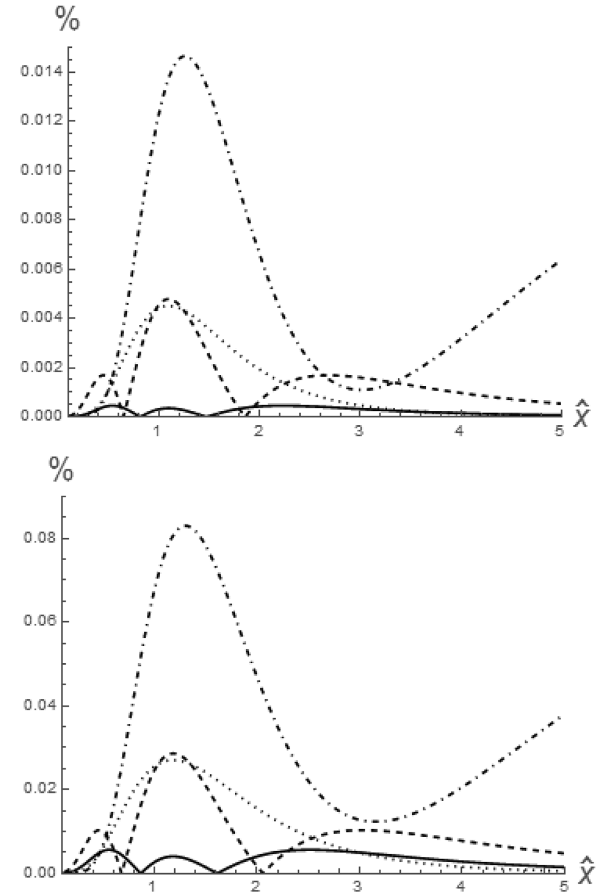

Figure 3 Relative traveltime error from non-hyperbolic approximations in VTI media with (top) $\eta = 0.1$ and (bottom) $\eta = 0.2$. The results from the GMA and Alkhalifah (2011) approximations and the first- and second-order Shanks transform (equation (8)) are shown as dotted, dash-dotted, dashed and solid lines, respectively. $\hat{x}$ is the normalised offset.

The perturbation series is defined by

$$\tau = a_0 + a_1\eta + a_2\eta^2, \tag{3}$$

where the series coefficients $a_j(x)$ can be found in Appendix A. The Shanks transform (Bender and Orszag 1978) is applied to the approximation presented in equation (3) to obtain a higher accuracy level.

In this paper, we propose an alternative hyperbolic background model:

$$t^2 \approx t_0^2 + \frac{x^2}{V_h^2}, \tag{4}$$

where V_h is the horizontal velocity with $V_h = V_0\sqrt{1+2\varepsilon} = V_n\sqrt{1+2\eta}$. Using the alternative background model means that, instead of vertical velocity V_0 and NMO velocity V_n (the curvature of slowness surface at zero horizontal slowness),

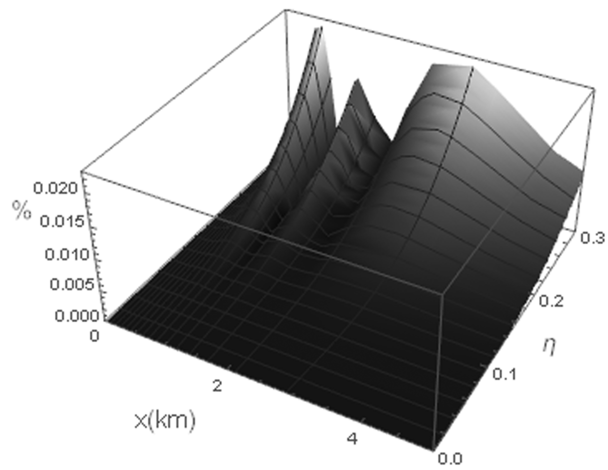

Figure 4 Relative traveltime error with offset and anellipticity parameter η using the second-order Shanks transform τ_{S2}.

we are using vertical velocity V_0 (or the vertical slowness) and horizontal velocity V_h (or the horizontal slowness) to represent the model as shown in Fig. 1.

The comparison between the hyperbolic moveout approximations (1) and (4) is illustrated in Fig. 2 for a VTI model with parameters: $V_0 = 2$ km/s, $t_0 = 0.5s$, $\delta = 0.1$ and $\eta = 0.1$. One can see that the new approximation is slightly worse for intermediate offsets but much better for large offsets.

To define the perturbation coefficients for a new background, we solve the VTI eikonal equation (Alkhalifah 2000) defined with horizontal velocity:

$$V_h^2\left(\frac{\partial\tau}{\partial x}\right)^2 + V_0^2\left(\frac{\partial\tau}{\partial z}\right)^2 - \frac{2\eta}{1+2\eta}V_h^2V_0^2\left(\frac{\partial\tau}{\partial x}\right)^2\left(\frac{\partial\tau}{\partial z}\right)^2 = 1. \tag{5}$$

Similar to equation (3), the new perturbation series up to the third order in η is defined as

$$\tau = \tau_0 + b_1\eta + b_2\eta^2 + b_3\eta^3. \tag{6}$$

Solving eikonal equation (5) for a homogeneous VTI medium results in the following coefficients (Appendix B):

$$\tau_0 = \sqrt{t_0^2 + \frac{x^2}{V_h^2}},$$

$$b_1 = \frac{t_0^2x^2}{\tau_0^3V_h^2},$$

$$b_2 = -\frac{9t_0^4x^4}{2\tau_0^7V_h^4},$$

$$b_3 = \frac{-8t_0^8V_h^4x^4 + 65t_0^6V_h^2x^6 - 8t_0^4x^8}{2\tau_0^{11}V_h^8}. \tag{7}$$

To improve the accuracy of the perturbation series in equation (6), we can use the first- and second-order Shanks transform (Bender and Orszag 1978), which gives

$$\tau_{S1} = \frac{\tau_0\tau_2 - \tau_1^2}{\tau_0 + \tau_2 - 2\tau_1},$$
$$\tau_{S2} = \frac{\tau_1\tau_3 - \tau_2^2}{\tau_1 + \tau_3 - 2\tau_2}, \quad (8)$$

where $\tau_k = \tau_0 + \sum_{j=1}^{k} b_j\eta^j$, $k = 1, 2, 3$.

Using the VTI model parameters introduced above, we compare the accuracy of the proposed approximations in equation (8) with other well-known approximations: GMA and Alkhalifah (2011) (Appendix A). The results are shown in Fig. 3 with different values for anellipticity parameter η. The relative error in traveltime is plotted versus normalised offset, $\hat{x} = x/(t_0 V_n)$. One can see that, regardless of the chosen values for η, the second-order Shanks transform from equation (8) gives the best accuracy, whereas the method by Alkhalifah (2011) is the worst one. The sensitivity analysis from the second-order Shanks transform τ_{S2} with anellipticity parameter η is shown in Fig. 4. The error is very small with a small value of η.

New moveout approximation in an orthorhombic model

We can also select the perturbation series in anellipticity parameters for the ORT case. Compared with the VTI model, different from the anellipticity parameters in Masmoudi and Alkhalifah (2016), three anellipticity parameters in the ORT model are η_1 and η_2 defined in two vertical symmetry planes $[X, Z]$ and $[Y, Z]$ and η_3 in horizontal plane $[X, Y]$ (Vasconcelos and Tsvankin 2006) or anellipticity parameters η_1 and η_2 defined in two vertical symmetry planes $[X, Z]$ and $[Y, Z]$ and one cross-term anelliptic parameter η_{xy} (Stovas 2015). With these parameterisations, we define different forms of the moveout approximation based on the selection of anellipticity parameters and elliptical background models shown in Table 1.

Table 1 Four types of parameterisations based on different background models and the perturbation parameters

Parameterisation	Background	Perturbation parameters
Case A	V_0, V_{n1}, V_{n2}	η_1, η_2, η_3
Case B	V_0, V_{n1}, V_{n2}	$\eta_1, \eta_2, \eta_{xy}$
Case C	V_0, V_{h1}, V_{h2}	η_1, η_2, η_3
Case D	V_0, V_{h1}, V_{h2}	$\eta_1, \eta_2, \eta_{xy}$

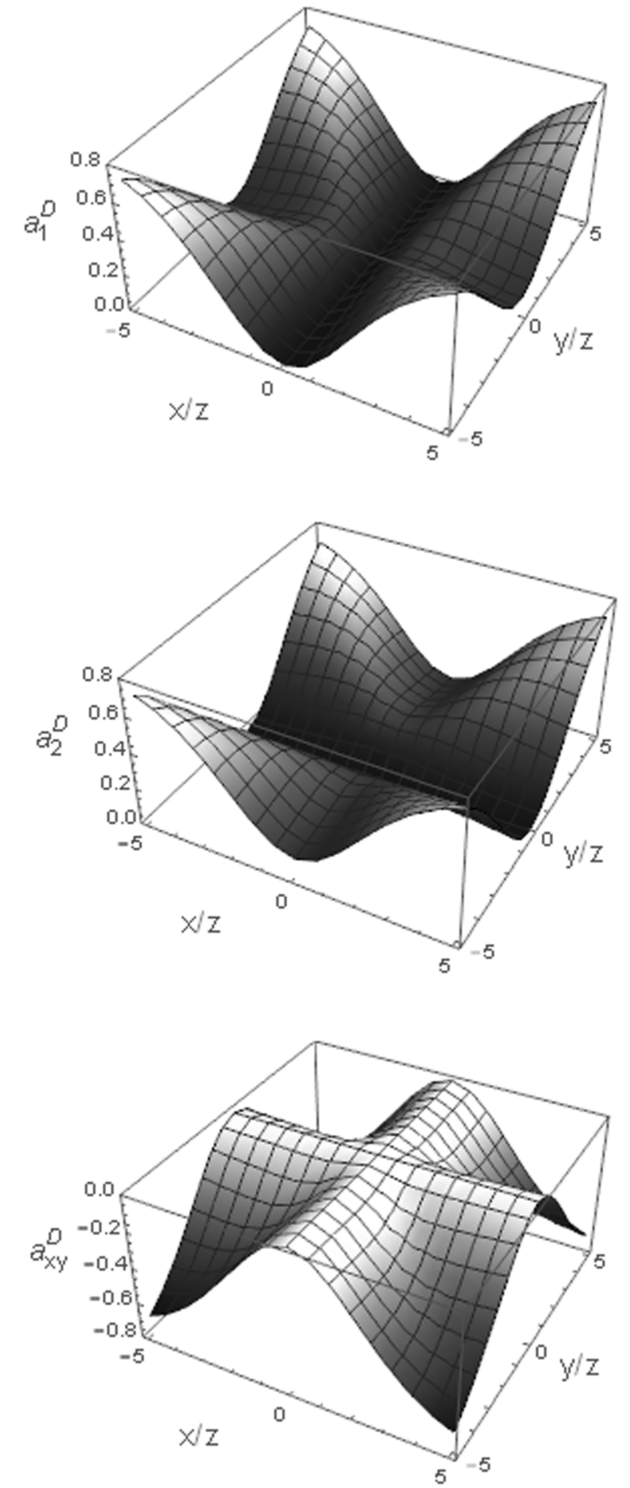

Figure 5 First-order coefficients (top) a_1^D, (middle) a_2^D and (bottom) a_{xy}^D computed from equation (C8) in the ORT model.

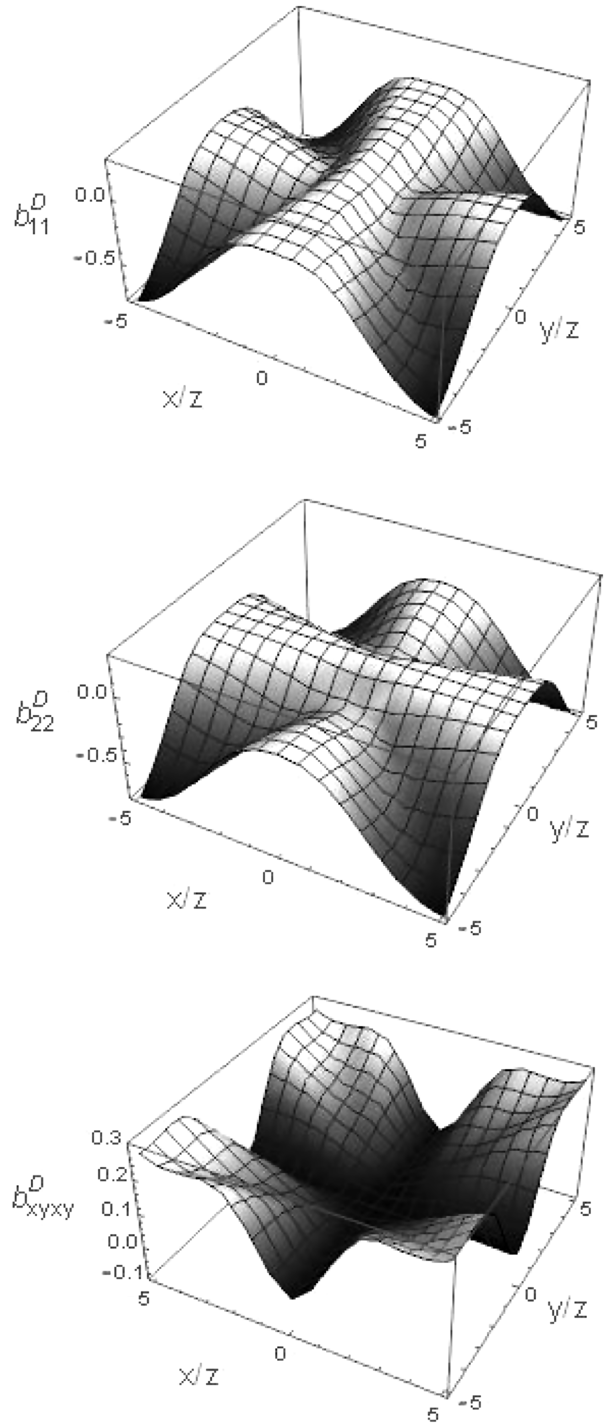

Figure 6 Second-order coefficients (top) b^D_{11}, (middle) b^D_{22} and (bottom) b^D_{xyxy} computed from equation (C8) in the ORT model.

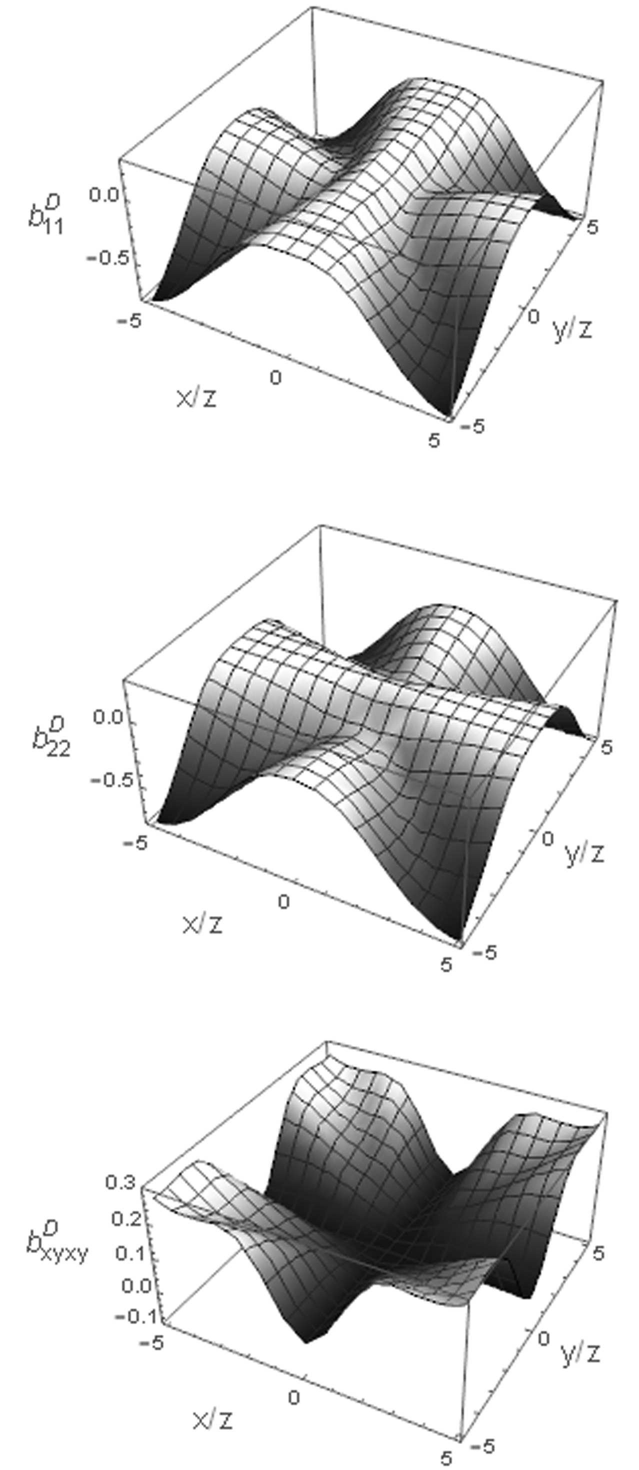

Figure 7 Cross-term coefficients (top) b^D_{12}, (middle) b^D_{1xy} and (bottom) b^D_{2xy} computed from equation (C8) in the ORT model.

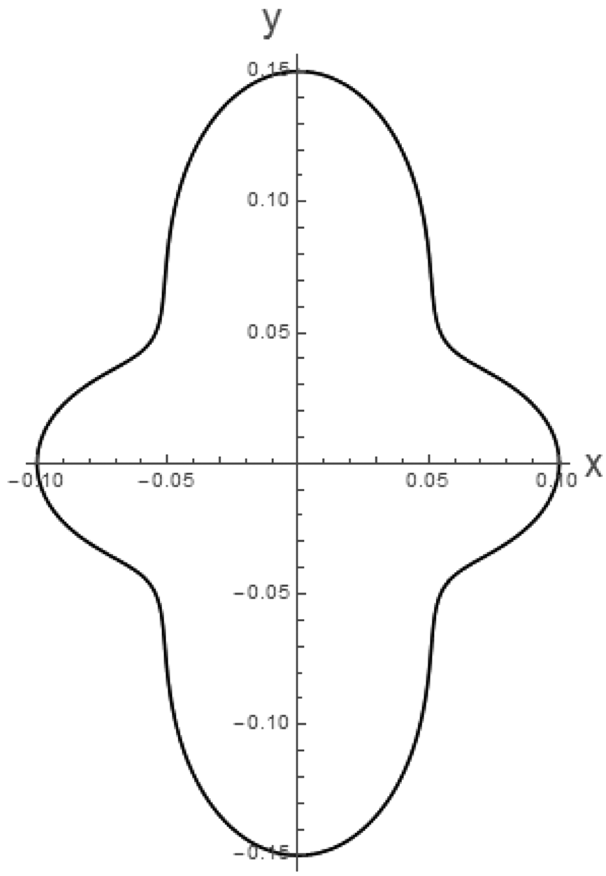

Figure 8 Azimuth-dependent anellipticity from equation (15) in the ORT model.

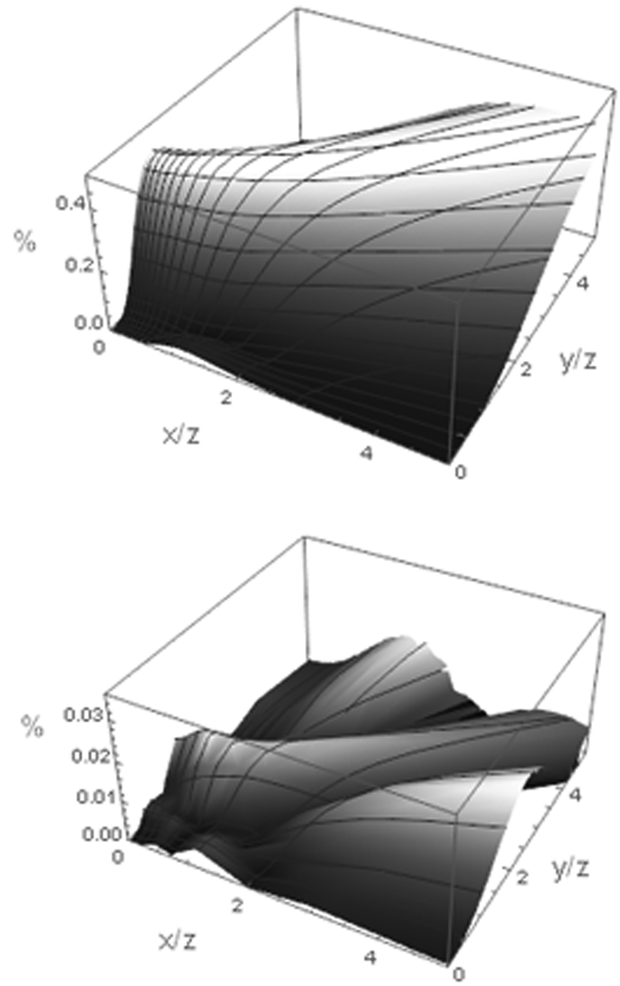

Figure 9 Relative traveltime error for the ORT model by using (top) the perturbation series approximation in equation (C7) and (bottom) the approximation after Shanks transform in equation (17).

The perturbation series in terms of anellipticity parameters is defined up to the second order (Stovas *et al.* 2016):

$$\tau = \tau_0 + \sum_i a_i^k \eta_i + \sum_{i,j} b_{ij}^k \eta_i \eta_j, \; k = A, B, C, D. \tag{9}$$

First, we define case A for the ORT medium by selecting the elliptical background model by V_0, V_{n1} and V_{n2} and the perturbation parameters η_1, η_2 and η_3.

We solve the ORT eikonal equation (Alkhalifah 2003) with NMO velocities:

$$\begin{aligned} & V_0^2\left(\frac{\partial\tau}{\partial z}\right)^2 + (1+2\eta_1)\,V_{n1}^2\left(\frac{\partial\tau}{\partial x}\right)^2 + (1+2\eta_2)\,V_{n2}^2\left(\frac{\partial\tau}{\partial y}\right)^2 \\ & - 2\eta_1 V_{n1}^2 V_0^2\left(\frac{\partial\tau}{\partial x}\right)^2\left(\frac{\partial\tau}{\partial z}\right)^2 - 2\eta_2 V_{n2}^2 V_0^2\left(\frac{\partial\tau}{\partial y}\right)^2\left(\frac{\partial\tau}{\partial z}\right)^2 \\ & - \left(\frac{(1+2\eta_1)(1+2\eta_2)\,2\eta_3}{1+2\eta_3}\right) V_{n1}^2 V_{n2}^2\left(\frac{\partial\tau}{\partial x}\right)^2\left(\frac{\partial\tau}{\partial y}\right)^2 \\ & + \left(4\eta_1\eta_2 - \left(\sqrt{\frac{(1+2\eta_1)(1+2\eta_2)}{1+2\eta_3}} - 1\right)^2\right) \\ & \times V_{n1}^2 V_{n2}^2 V_0^2\left(\frac{\partial\tau}{\partial x}\right)^2\left(\frac{\partial\tau}{\partial y}\right)^2\left(\frac{\partial\tau}{\partial z}\right)^2 = 1, \end{aligned} \tag{10}$$

where V_0, V_{n1} and V_{n2} are the vertical and the corresponding NMO velocities, respectively. Anellipticity parameters η_1, η_2 and η_3 are defined in corresponding two vertical symmetry planes and a horizontal plane, respectively. For the homogeneous ORT model, the series coefficients a_i^A and b_{ij}^A $(i, j = 1, 2, 3)$ are given in Appendix C.

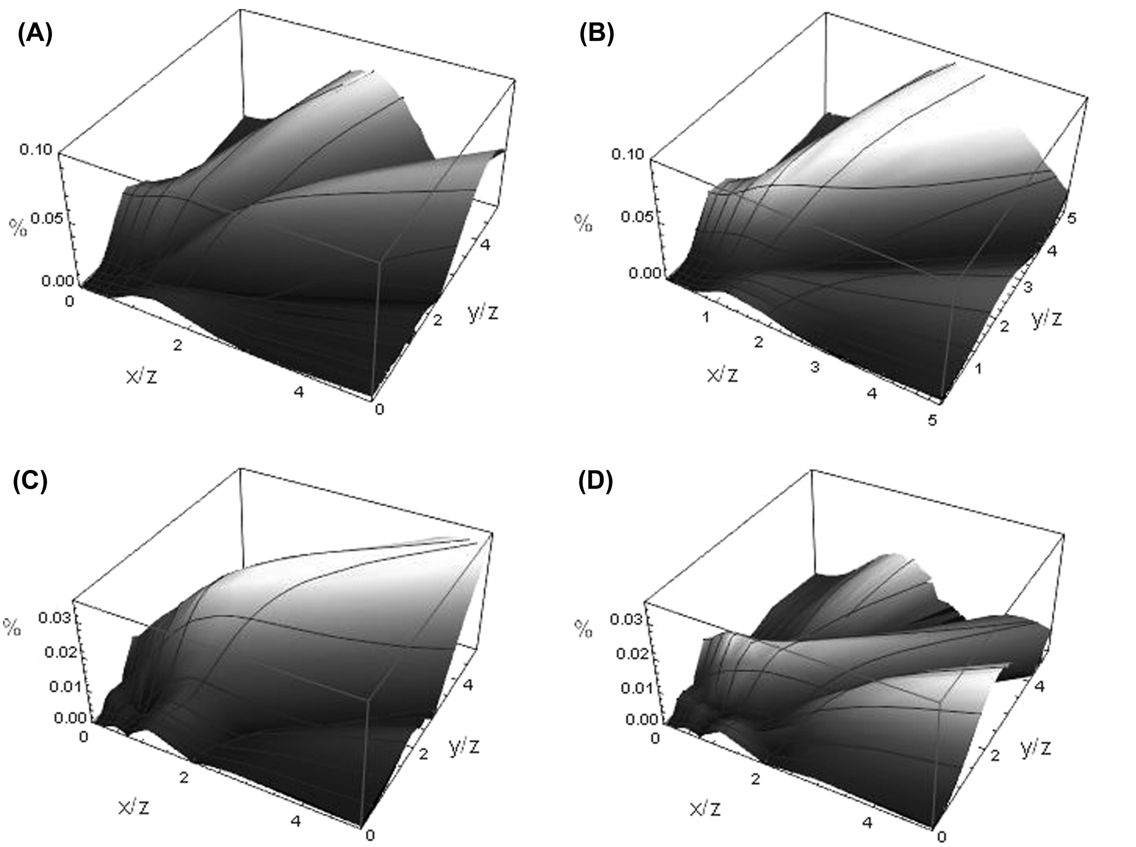

Figure 10 Relative traveltime error for the ORT model by using Shanks transform based on different parameterisations (cases A, B, C and D correspond to the ones specified in the main text).

We also define case B by selecting the elliptical background model by V_0, V_{n1} and V_{n2} and the cross-term anelliptic parameter η_{xy} defined by Stovas (2015):

$$\eta_{xy} = \sqrt{\frac{(1+2\eta_1)(1+2\eta_2)}{1+2\eta_3}} - 1. \tag{11}$$

The eikonal equation in this case takes the form of

$$\begin{aligned} &V_0^2\left(\frac{\partial \tau}{\partial z}\right)^2 + (1+2\eta_1)\, V_{n1}^2\left(\frac{\partial \tau}{\partial x}\right)^2 + (1+2\eta_2)\, V_{n2}^2\left(\frac{\partial \tau}{\partial y}\right)^2 \\ &- 2\eta_1 V_{n1}^2 V_0^2\left(\frac{\partial \tau}{\partial x}\right)^2\left(\frac{\partial \tau}{\partial z}\right)^2 - 2\eta_2 V_{n2}^2 V_0^2\left(\frac{\partial \tau}{\partial y}\right)^2\left(\frac{\partial \tau}{\partial z}\right)^2 \\ &- \left((1+2\eta_1)(1+2\eta_2) - \left(1+\eta_{xy}\right)^2\right) V_{n1}^2 V_{n2}^2\left(\frac{\partial \tau}{\partial x}\right)^2\left(\frac{\partial \tau}{\partial y}\right)^2 \\ &+ \left(4\eta_1\eta_2 - \eta_{xy}^2\right) V_{n1}^2 V_{n2}^2 V_0^2\left(\frac{\partial \tau}{\partial x}\right)^2\left(\frac{\partial \tau}{\partial y}\right)^2\left(\frac{\partial \tau}{\partial z}\right)^2 = 1. \end{aligned} \tag{12}$$

Solving the eikonal equation (12) with the corresponding perturbation series, we obtain the series coefficients a_i^B and b_{ij}^B $(i,\ j = 1, 2, xy)$ shown in Appendix C.

Similarly, we select another hyperbolic background model case with the horizontal velocities and reparameterise the ORT eikonal equation and solve it by using the corresponding perturbation series. The relation between horizontal and NMO velocities is given by $V_{hj} = V_{nj}\sqrt{1+2\eta_j}$, $j = 1, 2$, and the relation between η_3 and η_{xy} is given in equation (11).

We define case C by using V_0, V_{h1} and V_{h2} as the elliptical background model and the perturbation parameters by η_1, η_2 and η_3. The eikonal equation is given by

$$\begin{aligned} &V_0^2\left(\frac{\partial \tau}{\partial z}\right)^2 + V_{h1}^2\left(\frac{\partial \tau}{\partial x}\right)^2 + V_{h2}^2\left(\frac{\partial \tau}{\partial y}\right)^2 \\ &- \frac{2\eta_1}{1+2\eta_1} V_{h1}^2 V_0^2\left(\frac{\partial \tau}{\partial x}\right)^2\left(\frac{\partial \tau}{\partial z}\right)^2 - \frac{2\eta_2}{1+2\eta_2} V_{h2}^2 V_0^2\left(\frac{\partial \tau}{\partial y}\right)^2 \\ &\times\left(\frac{\partial \tau}{\partial z}\right)^2 - \frac{2\eta_3}{1+2\eta_3} V_{h1}^2 V_{h2}^2\left(\frac{\partial \tau}{\partial x}\right)^2\left(\frac{\partial \tau}{\partial y}\right)^2 \end{aligned}$$

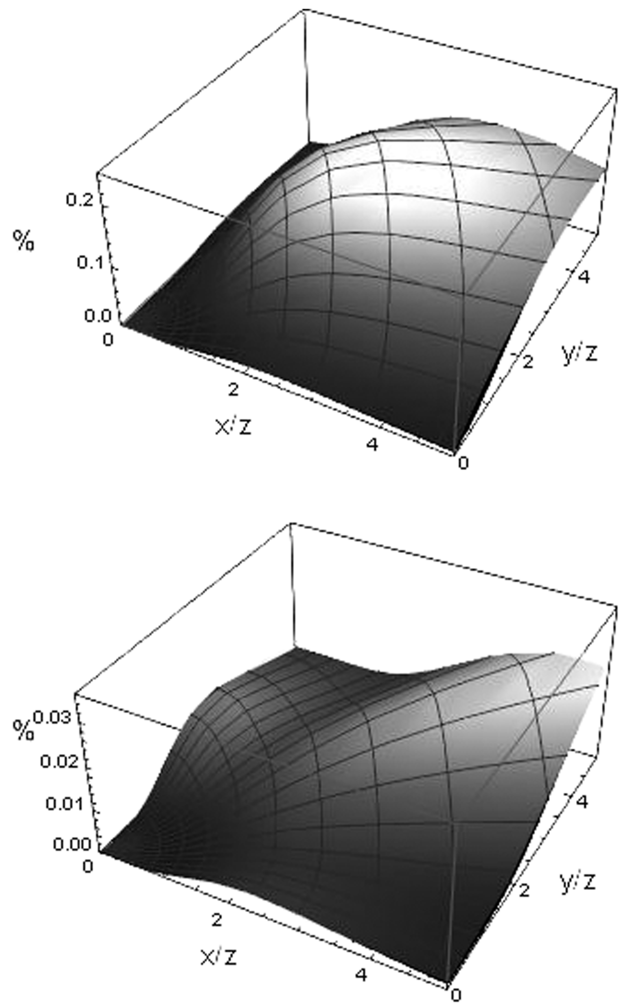

Figure 11 Relative traveltime error for the ORT model by using the approximations from (top) Sripanich and Fomel (2015) and (bottom) Hao and Stovas (2016).

$$
+\frac{4\eta_1\eta_2-\left(\sqrt{\frac{(1+2\eta_1)(1+2\eta_2)}{1+2\eta_3}}-1\right)^2}{(1+2\eta_1)(1+2\eta_2)}V_{h1}^2V_{h2}^2V_0^2\left(\frac{\partial\tau}{\partial x}\right)^2\left(\frac{\partial\tau}{\partial y}\right)^2\times\left(\frac{\partial\tau}{\partial z}\right)^2=1, \tag{13}
$$

and the corresponding series coefficients a_i^C and b_{ij}^C $(i,\ j=1,2,3)$ are shown in Appendix C.

For case D, we solve the ORT eikonal equation with horizontal velocities V_{h1} and V_{h2} and the perturbation parameters η_1, η_2 and η_{xy}:

$$
V_0^2\left(\frac{\partial\tau}{\partial z}\right)^2+V_{h1}^2\left(\frac{\partial\tau}{\partial x}\right)^2+V_{h2}^2\left(\frac{\partial\tau}{\partial y}\right)^2-\frac{2\eta_1}{1+2\eta_1}V_{h1}^2V_0^2\times\left(\frac{\partial\tau}{\partial x}\right)^2\left(\frac{\partial\tau}{\partial z}\right)^2-\frac{2\eta_2}{1+2\eta_2}V_{h2}^2V_0^2\left(\frac{\partial\tau}{\partial y}\right)^2\left(\frac{\partial\tau}{\partial z}\right)^2
$$
$$
-\frac{(1+2\eta_1)(1+2\eta_2)-(1+\eta_{xy})^2}{(1+2\eta_1)(1+2\eta_2)}V_{h1}^2V_{h2}^2\left(\frac{\partial\tau}{\partial x}\right)^2\left(\frac{\partial\tau}{\partial y}\right)^2
+\frac{4\eta_1\eta_2-\eta_{xy}^2}{(1+2\eta_1)(1+2\eta_2)}V_{h1}^2V_{h2}^2V_0^2\left(\frac{\partial\tau}{\partial x}\right)^2\left(\frac{\partial\tau}{\partial y}\right)^2\left(\frac{\partial\tau}{\partial z}\right)^2=1. \tag{14}
$$

The corresponding series coefficients a_i^D and b_{ij}^D $(i,\ j=1,2,xy)$ are shown in Appendix C.

To test the proposed method, we select case D as an example for the ORT model with the parameters: $t_0=0.5$s, $V_0=2$km/s, $V_{h1}=2.4$km/s ($V_{n1}=2.191$km/s), $V_{h2}=2.6$km/s ($V_{n2}=2.28$km/s), $\eta_1=0.1$, $\eta_2=0.15$ and $\eta_3=0.2(\eta_{xy}=0.0556)$. The coefficients $a_i^D, b_{ij}^D(i,k=1,2,xy)$ from equation (C8) are plotted in Figs. 5, 6 and 7. One can see that the first-order coefficients a_i^D (Fig. 5) are of the same magnitude, whereas the second-order diagonal coefficients b_{11}^D and b_{22}^D (Fig. 6) are slightly higher in magnitude comparing with coefficient b_{xyxy}^D. The cross-term coefficients b_{12}^D, b_{1xy}^D and b_{2xy}^D are smaller comparing with b_{11}^D, b_{22}^D and b_{xyxy}^D. Relatively large values of b_{1xy}^D and b_{2xy}^D at azimuth of $\pm\pi/4$ indicate the cross-talk between anelliptic parameters η_1 and η_{xy} and η_2 and η_{xy}, respectively.

The anellipticity in terms of azimuth is given by Stovas (2015):

$$
\eta_r(\Phi)=\frac{\frac{\eta_1\cos^4\Phi}{V_{n1}^4}+\frac{\eta_2\sin^4\Phi}{V_{n2}^4}+\frac{\eta_{xy}\sin^2\Phi\cos^2\Phi}{V_{n1}^2V_{n2}^2}}{\left(\frac{\cos^2\Phi}{V_{n1}^2}+\frac{\sin^2\Phi}{V_{n2}^2}\right)^2}, \tag{15}
$$

where the group azimuth is defined by

$$
\tan\Phi=\frac{y}{x}, \tag{16}
$$

with x and y being the corresponding projections of radial offset.

The azimuth-dependent anellipticity from equation (15) defined for the ORT model described above is shown in Fig. 8. We see that the anellipticity is very weak at the azimuth around $\pm\pi/4$ because the cross-term η_{xy} in this model is very small, which can be observed from coefficients b_{1xy}^D and b_{2xy}^D shown in Fig. 7.

To obtain a higher accuracy level, the Shanks transform (Bender and Orszag 1978) is applied for all these four cases defined in Table 1 by the form given by

$$\tau_3 = \frac{\tau_0 \tau_2 - \tau_1^2}{\tau_0 + \tau_2 - 2\tau_1}, \tag{17}$$

where τ_0 is defined in equation (C1), and $\tau_1 = \tau_0 + \sum_i a_i^k \eta_i$ and $\tau_2 = \tau_1 + b_{ij}^k \eta_i \eta_j$, $k = A, B, C, D$.

To demonstrate equation (17), we select case D and use the ORT model with parameters mentioned above. In Fig. 9 (top), one can see the relative error in the estimation of traveltime curves from the perturbation series approximation given in equation (C7). The relative error in the estimation of traveltime from approximation with the Shanks transform given by equation (17) is shown in Fig. 9 (bottom). One can see that the Shanks transform results in one-order improvement in traveltime accuracy.

Numerical examples

To compute the traveltime for the ORT model, we use exact parametric offset–traveltime equations (Stovas 2015):

$$x(p_x, p_y) = p_x F_2 \frac{V_{n1}^2 t_0}{f_1^{1/2} f_2^{3/2}},$$

$$y(p_x, p_y) = p_y F_1 \frac{V_{n2}^2 t_0}{f_1^{1/2} f_2^{3/2}},$$

$$t(p_x, p_y) = \frac{t_0 \left(F_1 p_y^2 V_{n2}^2 + F_2 p_x^2 V_{n1}^2 + f_1 f_2\right)}{f_1^{1/2} f_2^{3/2}}, \tag{18}$$

where x and y are the corresponding offset projections, p_x and p_y are the horizontal slowness defined in two vertical symmetry planes, and

$$\begin{aligned} F_1 &= \left(p_x^2 V_{n1}^2 (2\eta_1 - \eta_{xy}) - 1\right)^2, \\ F_2 &= \left(p_y^2 V_{n2}^2 (2\eta_2 - \eta_{xy}) - 1\right)^2, \\ f_1 &= 1 - (1 + 2\eta_1)\, p_x^2 V_{n1}^2 - (1 + 2\eta_2)\, p_y^2 V_{n2}^2 \\ &\quad + \left((1 + 2\eta_1)(1 + 2\eta_2) - \left(1 + \eta_{xy}\right)^2\right) p_x^2 p_y^2 V_{n1}^2 V_{n2}^2, \\ f_2 &= 1 - 2\eta_1 p_x^2 V_{n1}^2 - 2\eta_2 p_y^2 V_{n2}^2 + \left(4\eta_1 \eta_2 - \eta_{xy}^2\right) p_x^2 p_y^2 V_{n1}^2 V_{n2}^2. \end{aligned} \tag{19}$$

With the ORT model introduced above, the results of the Shanks transform applied for the perturbation series using these parameterisations are illustrated in Fig. 10. One can see that the results obtained with the Shanks transform in case A are very similar with the results obtained with the Shanks transform in case B, whereas the best results are obtained with the Shanks transform in cases C and D (with horizontal-velocity parameterisation). The detailed analysis indicates that case D results in slightly better accuracy comparing with case C results.

To compare our results with other well-known moveout approximations, we select the most accurate ones: from Sripanich and Fomel (2015) and Hao and Stovas (2016). The results from these approximations are shown in Fig. 11. One can see that the Sripanich–Fomel approximation is one order less accurate comparing with our best approximation, and the Hao–Stovas approximation is slightly worse in accuracy.

CONCLUSIONS

We developed a new moveout approximation based on the perturbation method with an alternative background model. We applied this approach for homogeneous vertical transverse isotropic and orthorhombic (ORT) media. We tested our approach with different parameterisations both for velocities and anelliptic parameters in the ORT model. The comparison between the results from the standard moveout approximations based on normal moveout velocities and two well-known moveout approximations shows that the application of our proposed approach with horizontal velocities as a background model results in better traveltime accuracy. The parameterisation with anelliptic parameters η_1, η_2, η_{xy} results in the best accuracy for traveltime estimation in the ORT model. The Shanks transform improves by almost one order in traveltime accuracy. This method is applied for a homogeneous model but can be extended for a multi-layered medium.

ACKNOWLEDGEMENTS

The authors would like to thank the China Scholarship Council (CSC) and the ROSE project for financial support.

REFERENCES

Alkhalifah T. 1998. Acoustic approximations for processing in transversely isotropic media. *Geophysics* **63**, 623–631.

Alkhalifah T. 2000. An acoustic wave equation for anisotropic media. *Geophysics* **65**, 1239–1250.

Alkhalifah T. 2003. An acoustic wave equation for orthorhombic anisotropy. *Geophysics* **68**, 1169–1172.

Alkhalifah T. 2011. Scanning anisotropy parameters in complex media. *Geophysics* **76**(2), U13–U22.

Bender C.M. and Orszag S.A. 1978. *Advanced Mathematical Methods for Scientists and Engineers*. McGraw-Hill.

Fomel S. 2004. On anelliptic approximations for qP velocities in VTI media. *Geophysical Prospecting* **52**, 247–259.

Fomel S. and Stovas A. 2010. Generalized nonhyperbolic moveout approximation. *Geophysics* **75**(2), U9–U18.
Fowler P.J. 2003. Practical VTI approximations: a systematic anatomy. *Journal of Applied Geophysics* **54**, 347–367.
Golikov P. and Stovas A. 2012. Accuracy comparison of nonhyperbolic moveout approximations for qP-waves in VTI media. *Journal of Geophysics and Engineering* **9**, 428–432.
Grechka V. and Tsvankin I. 1999a. 3-D moveout velocity analysis and parameter estimation for orthorhombic media. *Geophysics* **64**, 820–837.
Grechka V. and Tsvankin I. 1999b. 3-D moveout inversion in azimuthally anisotropic media with lateral velocity variation: theory and a case study. *Geophysics* **64**, 1202–1218.
Hao Q. and Stovas A. 2016. Analytic calculation of phase and group velocities of P-waves in orthorhomic media. *Geophysics* **81**(3), C79–C97.
Masmoudi N. and Alkhalifah T. 2016. Traveltime approximations and parameter estimation for orthorhombic media. *Geophysics* **81**(4), C127–C137.
Schoenberg M. and Helbig K. 1997. Orthorhombic media: modeling elastic wave behavior in a vertically fractured earth. *Geophysics* **62**, 1954–1974.
Sripanich Y. and Fomel S. 2015. On anelliptic approximations for qP velocities in transversely isotropic and orthorhombic media. *Geophysics* **80**(5), C89–C105.
Stovas A. 2015. Azimuthally dependent kinematic properties of orthorhombic media. *Geophysics* **80**(6), C107–C122.
Stovas A., Masmoudi N. and Alkhalifah T. 2016. Application of perturbation theory for P-wave eikonal equation in orthorhombic media. EAGE Conference and Exhibition, Vienna, Austria, Expanded Abstracts, Tu SBT5 15.
Thomsen L. 1986. Weak elastic anisotropy. *Geophysics* **51**, 1954–1966.
Tsvankin I. 1997. Anisotropic parameters and P-wave velocity for orthorhombic media. *Geophysics* **62**, 1292–1309.
Tsvankin I. 2012. Seismic signatures and analysis of reflection data in anisotropic media. In: *Geophysical References Series*, Vol. **19**. Society of Exploration Geophysicists.
Vasconcelos I. and Tsvankin I. 2006. Non-hyperbolic moveout inversion of wide-azimuth P-wave data for orthorhombic media. *Geophysical Prospecting* **54**, 535–552.

APPENDIX A

Fomel and Stovas (2010) proposed the generalised nonhyperbolic moveout approximation from the zero-offset ray and one additional nonzero-offset ray given by

$$
\begin{aligned}
t^2 &= t_0^2\left(1+\hat{x}^2-\frac{4\eta\hat{x}^4}{1+B\hat{x}^2+\sqrt{1+2B\hat{x}^2+C\hat{x}^4}}\right),\\
B &= \frac{1+8\eta+8\eta^2}{1+2\eta},\\
C &= \frac{1}{(1+2\eta)^2},
\end{aligned}
\tag{A1}
$$

where parameters B and C are set for an acoustic vertical transverse isotropic (VTI) medium, and $\hat{x}$ is the normalised offset defined by $\hat{x}=x/(t_0V_n)$.

Alkhalifah (2011) proposed to expand the traveltime expression into a series in anelliptic parameter η (Alkhalifah 1998) by solving the eikonal equation (Alkhalifah 2000), where $\eta=(\varepsilon-\delta)/(1+2\delta)$ with parameters δ and ε being the Thomsen anisotropy parameters (Thomsen 1986), as follows:

$$
\begin{aligned}
&V_n^2(1+2\eta)\left(\frac{\partial\tau}{\partial x}\right)^2+V_0^2\left(\frac{\partial\tau}{\partial z}\right)^2\\
&\quad-2\eta V_n^2V_0^2\left(\frac{\partial\tau}{\partial x}\right)^2\left(\frac{\partial\tau}{\partial z}\right)^2=1.
\end{aligned}
\tag{A2}
$$

The perturbation series is defined by

$$
\tau=a_0+a_1\eta+a_2\eta^2,
\tag{A3}
$$

where the series coefficients are

$$
\begin{aligned}
a_0 &= \tau_0\sqrt{1+\hat{x}^2},\\
a_1 &= -\tau_0\sqrt{1+\hat{x}^2}\frac{\hat{x}^4}{(1+\hat{x}^2)^2},\\
a_2 &= \tau_0\sqrt{1+\hat{x}^2}\frac{3\hat{x}^6(4+\hat{x}^2)}{2(1+\hat{x}^2)^4}.
\end{aligned}
\tag{A4}
$$

The Shanks transform is applied to the approximation presented in equation (A3) to obtain a higher accuracy level with the following form:

$$
\begin{aligned}
\tau &= \frac{A_0A_2-A_1^2}{A_0+A_2-2A_1},\\
A_0 &= a_0,\\
A_1 &= a_0+a_1\eta,\\
A_2 &= a_0+a_1\eta+a_2\eta^2.
\end{aligned}
\tag{A5}
$$

APPENDIX B

To derive the perturbation series for traveltime, we solve the eikonal equation for VTI media (Alkhalifah 2000) with horizontal velocity:

$$
V_h^2\left(\frac{\partial\tau}{\partial x}\right)^2+V_0^2\left(\frac{\partial\tau}{\partial z}\right)^2-\frac{2\eta}{1+2\eta}V_h^2V_0^2\left(\frac{\partial\tau}{\partial x}\right)^2\left(\frac{\partial\tau}{\partial z}\right)^2=1.
\tag{B1}
$$

A trial solution can be represented as a series expansion in parameter η from solving equation (B1) by the perturbation method:

$$\tau = \tau_0 + b_1\eta + b_2\eta^2 + b_3\eta^3, \tag{B2}$$

where b_j, $j = 1, 3$ are the coefficients of expansion.

The zero-order term τ_0 can be obtained by solving equation (B1) with $\eta = 0$:

$$\left(\frac{\partial \tau_0}{\partial z}\right)^2 V_0^2 + \left(\frac{\partial \tau_0}{\partial x}\right)^2 V_h^2 = 1. \tag{B3}$$

In succession, the first-order coefficient b_1 can be obtained by solving the following equation:

$$\frac{\partial \tau_0}{\partial z}\frac{\partial b_1}{\partial z} V_0^2 + \frac{\partial \tau_0}{\partial x}\frac{\partial b_1}{\partial x} V_h^2 = \left(\frac{\partial \tau_0}{\partial x}\frac{\partial \tau_0}{\partial z}\right)^2 V_h^2 V_0^2. \tag{B4}$$

The second-order coefficient b_2 can be computed from the following equation:

$$\begin{aligned} &2\left(\left(\frac{\partial \tau_0}{\partial x}\frac{\partial b_2}{\partial x}\right) V_h^2 + \left(\frac{\partial \tau_0}{\partial z}\frac{\partial b_2}{\partial z}\right) V_0^2\right) \\ &\quad = 4 V_0^2 V_h^2 \left(\frac{\partial \tau_0}{\partial x}\right)\left(\frac{\partial \tau_0}{\partial z}\right) \\ &\qquad \times \left(\frac{\partial \tau_0}{\partial z}\frac{\partial b_1}{\partial x} + \frac{\partial \tau_0}{\partial x}\left(\frac{\partial b_1}{\partial z} - \frac{\partial \tau_0}{\partial z}\right)\right) \\ &\qquad - \left(\left(\frac{\partial b_1}{\partial x}\right)^2 V_h^2 + \left(\frac{\partial b_1}{\partial z}\right)^2 V_0^2\right). \end{aligned} \tag{B5}$$

The third-order coefficient b_3 is computed from

$$\begin{aligned} &V_h^2\left(\frac{\partial \tau_0}{\partial x}\frac{\partial b_3}{\partial x}\right) + V_0^2\left(\frac{\partial \tau_0}{\partial z}\frac{\partial b_3}{\partial z}\right) = V_0^2 V_h^2\left(\left(\frac{\partial \tau_0}{\partial z}\right)^2\left(\frac{\partial b_1}{\partial x}\right)^2\right. \\ &\quad + 2\frac{\partial \tau_0}{\partial x}\frac{\partial \tau_0}{\partial z}\left(2\frac{\partial b_1}{\partial x}\frac{\partial b_1}{\partial z} + \frac{\partial \tau_0}{\partial z}\left(\frac{\partial b_2}{\partial x} - 2\frac{\partial b_1}{\partial x}\right)\right) \\ &\quad \left. + \left(\frac{\partial \tau_0}{\partial x}\right)^2\left(2\frac{\partial \tau_0}{\partial z}\frac{\partial b_2}{\partial z} + \left(\frac{\partial b_1}{\partial z} - 2\frac{\partial \tau_0}{\partial z}\right)^2\right)\right) \\ &\quad - \left(\left(\frac{\partial b_1}{\partial z}\frac{\partial b_2}{\partial z}\right) V_0^2 + \left(\frac{\partial b_1}{\partial x}\frac{\partial b_2}{\partial x}\right) V_h^2\right). \end{aligned} \tag{B6}$$

For a homogeneous VTI medium, these coefficients can be explicitly computed as

$$\begin{aligned} \tau_0 &= \sqrt{t_0^2 + \frac{x^2}{V_h^2}}, \\ b_1 &= \frac{t_0^2 x^2}{\tau_0^3 V_h^2}, \\ b_2 &= -\frac{9 t_0^4 x^4}{2\tau_0^7 V_h^4}, \\ b_3 &= \frac{-t_0^4 x^4\left(8 t_0^4 V_h^4 - 65 t_0^2 V_h^2 x^2 + 8x^4\right)}{2\tau_0^{11} V_h^8}. \end{aligned} \tag{B7}$$

APPENDIX C

We can select different parameterisations for both velocities and anellipticity parameters. We use the following parameterisation cases shown in Table 1: (V_0, V_{n1}, V_{n2}, η_1, η_2, η_3, case A), (V_0, V_{n1}, V_{n2}, η_1, η_2, η_{xy}, case B), (V_0, V_{h1}, V_{h2}, η_1, η_2, η_3, case C) and (V_0, V_{h1}, V_{h2}, η_1, η_2, η_{xy}, case D). To compute the perturbation coefficients, we have to reparameterise the orthorhombic (ORT) eikonal equation and solve it by using the corresponding perturbation series shown in equation (9).

Using the standard elliptical background model with vertical and normal moveout (NMO) velocities and anellipticity parameters η_1, η_2 and η_3, the perturbation series for the ORT model (Case A) is defined by

$$\tau = \tau_0 + \sum_i a_i^A \eta_i + \sum_{i,j} b_{ij}^A \eta_i \eta_j, \quad i, j = 1, 2, 3. \tag{C1}$$

For a homogeneous ORT model, coefficients a_i^A and b_{ij}^A are computed from equation (10) and given by

$$\begin{aligned} \tau_0 &= \sqrt{t_0^2 + \tau_{nx}^2 + \tau_{ny}^2}, \\ a_1^A &= -\frac{\tau_{nx}^2\left(\tau_{nx}^2 + \tau_{ny}^2\right)}{\tau_0^3}, \\ a_2^A &= -\frac{\tau_{ny}^2\left(\tau_{nx}^2 + \tau_{ny}^2\right)}{\tau_0^3}, \\ a_3^A &= \frac{\tau_{nx}^2 \tau_{ny}^2}{\tau_0^3}, \end{aligned}$$

$$b_{11}^{A} = \frac{\tau_{nx}^2 \left(t_0^4 \tau_{ny}^2 + \left(\tau_{nx}^2 + \tau_{ny}^2\right)^2 \left(3\tau_{nx}^2 + 4\tau_{ny}^2\right) + t_0^2 \left(12\tau_{nx}^4 + 17\tau_{nx}^2\tau_{ny}^2 + 5\tau_{ny}^4\right)\right)}{2\tau_0^7},$$

$$b_{22}^{A} = \frac{\tau_{ny}^2 \left(t_0^4 \tau_{nx}^2 + \left(\tau_{nx}^2 + \tau_{ny}^2\right)^2 \left(3\tau_{ny}^2 + 4\tau_{nx}^2\right) + t_0^2 \left(12\tau_{ny}^4 + 17\tau_{nx}^2\tau_{ny}^2 + 5\tau_{nx}^4\right)\right)}{2\tau_0^7},$$

$$b_{33}^{A} = -\frac{3\tau_{nx}^2\tau_{ny}^2 \left(t_0^4 + 3\tau_{nx}^2\tau_{ny}^2 + t_0^2\left(\tau_{nx}^2 + \tau_{ny}^2\right)\right)}{2\tau_0^7},$$

$$b_{12}^{A} = -\frac{\tau_{nx}^2\tau_{ny}^2 \left(t_0^4 + \left(\tau_{nx}^2 + \tau_{ny}^2\right)^2 - 7t_0^2\left(\tau_{nx}^2 + \tau_{ny}^2\right)\right)}{\tau_0^7},$$

$$b_{13}^{A} = \frac{\tau_{nx}^2\tau_{ny}^2 \left(t_0^4 + \tau_{nx}^4 - \tau_{nx}^2\tau_{ny}^2 - 2\tau_{ny}^4 - t_0^2\left(7\tau_{nx}^2 + \tau_{ny}^2\right)\right)}{\tau_0^7},$$

$$b_{23}^{A} = \frac{\tau_{nx}^2\tau_{ny}^2 \left(t_0^4 + \tau_{ny}^4 - \tau_{nx}^2\tau_{ny}^2 - 2\tau_{x}^4 - t_0^2\left(7\tau_{ny}^2 + \tau_{nx}^2\right)\right)}{\tau_0^7}, \quad \text{(C2)}$$

where $\tau_{nx} = x/V_{n1}$ and $\tau_{ny} = y/V_{n2}$.

Using the standard elliptical background model with vertical and NMO velocities and anellipticity parameters η_1,η_2 and η_{xy}, the perturbation series for the ORT model (Case B) is defined by

$$\tau = \tau_0 + \sum_i a_i^B \eta_i + \sum_{i,j} b_{ij}^B \eta_i \eta_j, i, j = 1, 2, xy. \quad \text{(C3)}$$

For a homogeneous ORT model, coefficients a_i^B and b_{ij}^B are computed from equation (12) and given by

$$\tau_0 = \sqrt{t_0^2 + \tau_{nx}^2 + \tau_{ny}^2},$$

$$a_1^B = -\frac{\tau_{nx}^4}{\tau_0^3},$$

$$a_2^B = -\frac{\tau_{ny}^4}{\tau_0^3},$$

$$a_{xy}^B = -\frac{\tau_{nx}^2\tau_{ny}^2}{\tau_0^3},$$

$$b_{11}^B = \frac{3\tau_{nx}^6\left(4t_0^2 + 4\tau_{ny}^2 + \tau_{nx}^2\right)}{2\tau_0^7},$$

$$b_{22}^B = \frac{3\tau_{ny}^6\left(4t_0^2 + 4\tau_{nx}^2 + \tau_{ny}^2\right)}{2\tau_0^7},$$

$$b_{xyxy}^B = \frac{3\tau_{nx}^2\tau_{ny}^2\left(\tau_{nx}^4 - \tau_{nx}^2\tau_{ny}^2 + \tau_{ny}^4 + t_0^2\left(\tau_{nx}^2 + \tau_{ny}^2\right)\right)}{2\tau_0^7},$$

$$b_{12}^B = -\frac{9\tau_{nx}^4\tau_{ny}^4}{\tau_0^7},$$

$$b_{1xy}^B = \frac{3\tau_{nx}^4\tau_{ny}^2\left(2t_0^2 - \tau_{nx}^2 + 2\tau_{ny}^2\right)}{\tau_0^7},$$

$$b_{2xy}^B = \frac{3\tau_{ny}^4\tau_{nx}^2\left(2t_0^2 - \tau_{ny}^2 + 2\tau_{nx}^2\right)}{\tau_0^7}. \quad \text{(C4)}$$

Using the elliptical background model with vertical and horizontal velocities and anellipticity parameters η_1,η_2 and η_3, the perturbation series for the ORT model (Case C) is defined by

$$\tau = \tau_0 + \sum_i a_i^C \eta_i + \sum_{i,j} b_{ij}^C \eta_i \eta_j, i, j = 1, 2, 3. \quad \text{(C5)}$$

For a homogeneous ORT model, coefficients a_i^C and b_{ij}^C are computed from equation (13) and given by

$$\tau_0 = \sqrt{t_0^2 + \tau_{hx}^2 + \tau_{hy}^2},$$

$$a_1^C = \frac{t_0^2\tau_{hx}^2}{\tau_0^3},$$

$$a_2^C = \frac{t_0^2\tau_{hy}^2}{\tau_0^3},$$

$$a_3^C = \frac{\tau_{hx}^2\tau_{hy}^2}{\tau_0^3},$$

$$b_{11}^C = -\frac{3t_0^2\tau_{hx}^2\left(\tau_{hy}^2\left(\tau_{hx}^2 + \tau_{hy}^2\right) + t_0^2\left(3\tau_{hx}^2 + \tau_{hy}^2\right)\right)}{2\tau_0^7},$$

$$b_{22}^C = -\frac{3t_0^2\tau_{hy}^2\left(\tau_{hx}^2\left(\tau_{hx}^2 + \tau_{hy}^2\right) + t_0^2\left(3\tau_{hy}^2 + \tau_{hx}^2\right)\right)}{2\tau_0^7},$$

$$b_{33}^C = -\frac{3\tau_{hx}^2\tau_{hy}^2\left(t_0^4 + 3\tau_{hx}^2\tau_{hy}^2 + t_0^2\left(\tau_{hx}^2 + \tau_{hy}^2\right)\right)}{2\tau_0^7},$$

$$b_{12}^C = \frac{3t_0^2\tau_{hx}^2\tau_{hy}^2\left(\tau_{hx}^2 + \tau_{hy}^2 - 2t_0^2\right)}{\tau_0^7},$$

$$b_{13}^C = \frac{3t_0^2\tau_{hx}^2\tau_{hy}^2\left(\tau_{hy}^2 - 2\tau_{hx}^2 + t_0^2\right)}{\tau_0^7},$$

$$b_{23}^C = \frac{3t_0^2\tau_{hx}^2\tau_{hy}^2\left(\tau_{hx}^2 - 2\tau_{hy}^2 + t_0^2\right)}{\tau_0^7}, \tag{C6}$$

where $\tau_{hx} = x/V_{h1}$ and $\tau_{hy} = y/V_{h2}$.

Using the elliptical background model with vertical and horizontal velocities and anellipticity parameters η_1,η_2 and η_{xy}, the perturbation series for the ORT model (Case D) is defined by

$$\tau = \tau_0 + \sum_i a_i^D\eta_i + \sum_{i,j} b_{ij}^D\eta_i\eta_j, \quad i,\, j = 1, 2, xy. \tag{C7}$$

For a homogeneous ORT model, coefficients a_i^D and b_{ij}^D are computed from equation (14) and given by

$$\tau_0 = \sqrt{t_0^2 + \tau_{hx}^2 + \tau_{hy}^2},$$

$$a_1^D = \frac{\tau_{hx}^2\left(t_0^2 + \tau_{hy}^2\right)}{\tau_0^3},$$

$$a_2^D = \frac{\tau_{hy}^2\left(t_0^2 + \tau_{hx}^2\right)}{\tau_0^3},$$

$$a_{xy}^D = -\frac{\tau_{hx}^2\tau_{hy}^2}{\tau_0^3},$$

$$b_{11}^D = -\frac{9\tau_{hx}^4\left(t_0^2 + \tau_{hy}^2\right)^2}{2\tau_0^7},$$

$$b_{22}^D = -\frac{9\tau_{hy}^4\left(t_0^2 + \tau_{hx}^2\right)^2}{2\tau_0^7},$$

$$b_{xyxy}^D = \frac{3\tau_{hx}^2\tau_{hy}^2}{2\tau_0^7}\left(\tau_{hx}^4 + \tau_{hy}^4 - \tau_{hx}^2\tau_{hy}^2 + t_0^2\left(\tau_{hx}^2 + \tau_{hy}^2\right)\right),$$

$$b_{12}^D = \frac{\tau_{hx}^2\tau_{hy}^2}{\tau_0^7}\left(2\tau_{hx}^4 + 2\tau_{hy}^4 - t_0^4 - 5\tau_{hx}^2\tau_{hy}^2 + t_0^2\left(\tau_{hx}^2 + \tau_{hy}^2\right)\right),$$

$$b_{1xy}^D = -\frac{\tau_{hx}^2\tau_{hy}^2}{\tau_0^7}\left(2\tau_{hx}^4 + 2\tau_{hy}^4 + 2t_0^4 - 5\tau_{hx}^2\tau_{hy}^2 + t_0^2\left(4\tau_{hy}^2 - 5\tau_{hx}^2\right)\right),$$

$$b_{2xy}^D = -\frac{\tau_{hx}^2\tau_{hy}^2}{\tau_0^7}\left(2\tau_{hx}^4 + 2\tau_{hy}^4 + 2t_0^4 - 5\tau_{hx}^2\tau_{hy}^2 + t_0^2\left(4\tau_{hx}^2 - 5\tau_{hy}^2\right)\right). \tag{C8}$$